STATE OF THE CLIMATE IN 2016

Special Supplement to the
Bulletin of the American Meteorological Society
Vol. 98, No. 8, August 2017

status before rapidly decaying due to high wind shear. It did not cause any notable damage.

Just six weeks after TC Winston destroyed parts of Fiji, Major Tropical Cyclone Zena passed to the south of the country on April 4. Zena peaked as a category 3 Major TC, with 10-minute sustained winds measuring 70 kt (36.1 m s^{-1}) and central pressure 975 hPa at its lowest. Zena caused flooding in parts of Fiji but no significant damage. After passing Fiji, Zena traveled to Tonga where it caused heavy rain.

The last named tropical cyclone of the 2015/16 season was Major Tropical Cyclone Amos. Amos was first noted as a tropical disturbance on 13 April, when it was located to the northwest of Rotuma. The precursor to Major TC Amos caused flooding in Vanua Levu, Fiji, followed by very heavy rain and large waves in Wallis and Futuna after the storm achieved named TC status. The system subsequently moved southeast over Fiji on 16 April. After passing over Fiji, the system developed further as it moved northeast toward Samoa. The depression moved northwest toward Tuvalu and passed between the islands of Wallis and Futuna. Amos was named on 20 April and rapidly intensified as it moved east toward the Samoan Islands. Amos peaked as a category 3 Major TC, with 10-minute sustained wind speeds of 81 kt (41.7 m s^{-1}) during 22 April. Amos passed very close to or over Samoa during 23 April and then degraded into a tropical disturbance on 25 April. In Savai'i (Samoa), roads were damaged due to flooding, and approximately 70% of Samoa's population lost power during TC Amos due to high winds.

g. Tropical cyclone heat potential—G. J. Goni, J. A. Knaff, and I-I Lin

This section summarizes the changes in upper ocean thermal conditions within the seven tropical cyclone (TC) basins, using the tropical cyclone heat potential (TCHP; Goni and Trinanes 2003), a measure of the vertically-integrated upper ocean temperature conditions. The TCHP, defined as the excess heat content contained in the water column between the sea surface and the depth of the 26°C isotherm, has been linked to TC intensity changes (Shay et al. 2000; Goni and Trinanes 2003; I-I Lin et al. 2014) when favorable atmospheric conditions are also in place. In addition, the magnitude of the TCHP has also been identified as impacting the maximum potential intensity (Emanuel 1986; Bister and Emanuel 1998) through the modulating effect of the SST underlying the TC air–sea coupling (Mainelli et al. 2008; Lin et al. 2013). In general, fields of TCHP show high spatial and temporal variability associated mainly with oceanic mesoscale features and interannual variability (e.g., ENSO), or long-term decadal variability. This variability can be identified using satellite altimetry and in situ observations (Goni et al. 1996; Lin et al. 2008; Goni and Knaff 2009; Pun et al. 2013; Domingues et al. 2015), similar to analyses of meridional heat transport in the Atlantic Ocean (Dong et al. 2015).

To examine the TCHP year-to-year variability, two fields are presented here: 1) the TCHP anomalies (departures from the 1993–2015 mean values) during the months of TC activity in each hemisphere: June–November in the Northern Hemisphere, and November–April in the Southern Hemisphere, which generally show large variability within and among the TC basins (Fig. 4.39); and 2) differences of TCHP between the most recent (2016) and the previous TC season in 2015 (Fig. 4.40).

Most basins exhibited positive TCHP anomalies (Fig. 4.39), except for a small region just east of the date line in the South Pacific basin, providing anomalously favorable ocean conditions for the intensification of tropical cyclones. The western North Pacific basin is characterized by an increase in TCHP of ~ 10%–20% over the long-term average, as it recovered from the reduction of TCHP during the 2015 El Niño event (Zheng et al. 2015). Intrusions of the Loop Current in the Gulf of Mexico contribute to the generation of deep warm eddies, characterized by large TCHP values. The TCHP in the western Gulf

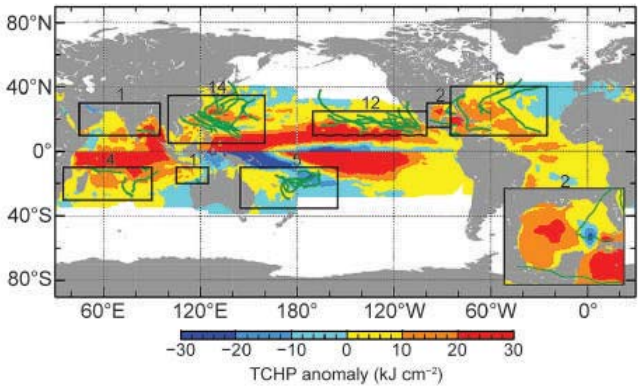

Fig. 4.39. Global anomalies of TCHP (kJ cm^{-2}) for Jun–Nov 2016 in the NH and Nov–Apr 2015/16 in the SH as described in the text. The boxes indicate 7 regions where TCs occur: from left to right, Southwest Indian, North Indian, West Pacific, Southeast Indian, South Pacific, East Pacific, and North Atlantic (shown as Gulf of Mexico and tropical Atlantic separately). Green lines indicate the trajectories of all tropical cyclones reaching at least category 1 and above during Jun–Nov 2016 in the NH and Nov 2015–Apr 2016 in the SH. Numbers above each box correspond to the number of category 1 and above cyclones that traveled within each box. Gulf of Mexico conditions during Jun–Nov 2016 are shown in the inset in the lower right corner.

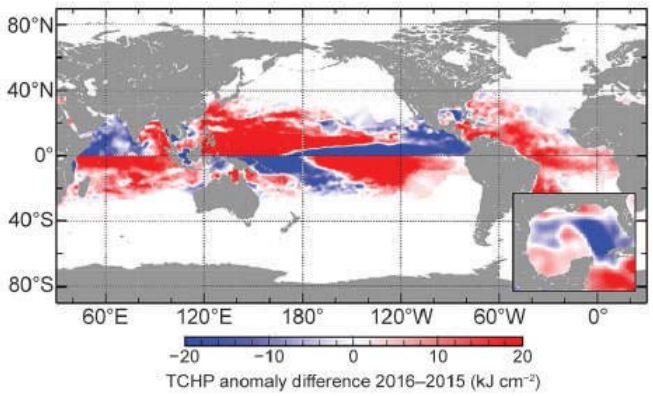

Fig. 4.40. Differences between the TCHP (kJ cm^{-2}) fields in 2016 and 2015 tropical cyclone seasons (Jun–Nov in the NH, and Nov–Apr in the SH).

of Mexico was again dominated by large positive anomalies, probably due to such eddies, while the eastern Gulf of Mexico exhibited lower values of TCHP, mainly due to a smaller-than-usual intrusion of the Loop Current into the Gulf of Mexico. Unlike 2015, when the Gulf of Mexico did not register any hurricanes, this season had two hurricanes traveling in the area. One storm (before it was named Hermine) moved directly over the largest negative anomalies as a tropical depression and later intensified when traveling over positive anomalies of TCHP.

In the ENP basin the positive TCHP anomalies are dominated by the strong El Niño conditions observed during early 2016 and a continued positive phase of the Pacific decadal oscillation (Zhang et al. 1997). The combination of these two phenomena is manifest in positive SST anomalies in that region and extending beyond the date line. Consequently, the TCHP values during the last season were even higher than average (Fig. 4.39). As was the case in 2014 and 2015, positive TCHP and SST anomalies contributed to elevated tropical cyclone activity, with 12 hurricanes in the eastern North Pacific during 2016 (Fig. 4.39).

The western North Pacific basin also usually exhibits anomalies related to ENSO variability (I-I Lin et al. 2014; Zheng et al. 2015). From the 1990s to 2013 it experienced a long-term decadal surface and subsurface warming associated with La Niña-like conditions (Pun et al. 2013; England et al. 2014; Lin and Chan 2015). However, the development of El Niño in late 2014 resulted in a pause in this warming trend. Since 2015, the strongest El Niño year since 1997, the TCHP over the WNP MDR (4°–19°N, 122°E–180°) fell considerably, as characterized by evident negative anomalies (Zheng et al. 2015; Goni et al. 2016). With the fading of El Niño in 2016 and the weak development of La Niña in the second half of the year, TCHP has recovered and shows positive anomalies again (Figs. 4.39, 4.40).

Supertyphoon Meranti's intensity reached 165 kt (85 m s^{-1}) and was the most intense TC globally in 2016. Meranti was only 5 kt (2.6 m s^{-1}) weaker than Supertyphoon Haiyan (2013). Both Meranti and Haiyan (I-I Lin et al. 2014) intensified over very favorable ocean conditions of TCHP ~130 kJ cm^{-2} (Lin et al. 2013; for additional details see Sidebar 4.2). Supertyphoon Nepartak was one of the most intense "first-appearing TC" of the season in recorded history—with its genesis in the month of July, Nepartak rapidly intensified while traveling over very warm water (TCHP ~120 kJ cm^{-2}) to its peak intensity of 150 kt (77 m s^{-1}) on 6 July. It then made landfall in Taiwan. Further details on Meranti and Nepartak can be found in Section 4f4 and Sidebar 4.2.

The 2016 season was noteworthy for several reasons with respect to intensification of tropical cyclones, including Supertyphoon Meranti in the western North Pacific and Hurricane Matthew in the tropical Atlantic basin, which was the costliest hurricane since Hurricane Sandy in 2012. The exact role that the oceans played in tropical storm intensification, however, requires more in-depth investigation.

h. Indian Ocean dipole—J.-J. Luo

The Indian Ocean dipole (IOD) represents a major mode of year-to-year climate variability in the tropical Indian Ocean (IO). The IOD shows a strong phase-locking with the seasonal cycle of Australian–East Asian monsoonal winds. The IOD usually starts in boreal summer, peaks in NH fall, and decays rapidly in early boreal winter. While IOD-related SST anomalies are generally weak and more localized compared to ENSO, the IOD can also cause large climate anomalies in many regions and play an active role in tropical interbasin interactions (e.g., Luo et al. 2010, 2012). During May–December 2016, a negative IOD (nIOD) occurred, six years after the last nIOD event in 2010 (Luo 2011). Compared to the previous seven negative events over the past 35 years (i.e., 1990, 1992, 1996, 1998, 2001, 2005, and 2010), the 2016 nIOD was fairly strong (Fig. 4.41). The IOD index during September–November 2016 reached −0.95°C, only slightly below the strongest nIOD in 1998 (−0.97°C). The 2016 nIOD event may have contributed to the flooding during boreal summer–fall in Indonesia and a persistent wet–cool austral spring in southeastern Australia (www.bom.gov.au/climate/iod/#tabs=Negative-IOD-impacts).

In 2016, as with the previous two strong nIOD events in 1998 and 2010, a strong El Niño occurred in the boreal winter of 2015/16 followed by a La Niña event. (Fig. 4.41). As a result of a delayed response